The Small Subunit of Carbamoyl Phosphate Synthetase: Snapshots along the Reaction Pathway†

James B. Thoden,‡ Xinyi Huang,§ Frank M. Raushel,§ and Hazel M. Holden*,‡

Department of Biochemistry, University of Wisconsin−Madison, 1710 University Avenue, Madison, Wisconsin, 53705, and Department of Chemistry, Texas A&M University, College Station, Texas, 77843

ABSTRACT: Carbamoyl phosphate synthetase (CPS) plays a key role in both arginine and pyrimidine biosynthesis by catalyzing the production of carbamoyl phosphate. The enzyme from *Escherichi coli* consists of two polypeptide chains referred to as the small and large subunits. On the basis of both amino acid sequence analyses and X-ray structural studies, it is known that the small subunit belongs to the Triad or Type I class of amidotransferases, all of which contain a cysteine−histidine (Cys269 and His353) couple required for activity. The hydrolysis of glutamine by the small subunit has been proposed to occur via two tetrahedral intermediates and a glutamyl-thioester moiety. Here, we describe the three-dimensional structures of the C269S/glutamine and CPS/glutamate γ-semialdehyde complexes, which serve as mimics for the Michaelis complex and the tetrahedral intermediates, respectively. In conjunction with the previously solved glutamyl-thioester intermediate complex, the stereochemical course of glutamine hydrolysis in CPS has been outlined. Specifically, attack by the thiolate of Cys269 occurs at the *Si* face of the carboxamide group of the glutamine substrate leading to a tetrahedral intermediate with an *S*-configuration. Both the backbone amide groups of Gly241 and Leu270, and O^{γ} of Ser47 play key roles in stabilizing the developing oxyanion. Collapse of the tetrahedral intermediate leads to formation of the glutamyl-thioester intermediate, which is subsequently attacked at the *Si* face by an activated water molecule positioned near His353. The results described here serve as a paradigm for other members of the Triad class of amidotranferases.

There are two general classes of amidotransferase enzymes that utilize glutamine as a precursor for the in situ generation of ammonia (*1*). These enzymes have evolved to capture the ammonia by an acceptor substrate prior to the release of this intermediate into the bulk solution. Carbamoyl phosphate synthetase, hereafter referred to as CPS,[1,2] is the best-characterized example of the Triad or *trpG*-type class of amidotransferases (*2*). In this family of enzymes, which also includes GMP synthetase, imidazole glycerol phosphate synthase, anthranilate synthase, and NAD synthetase, among others, there is a conserved trio of residues that is critical for the catalytic hydrolysis of glutamine and the production of ammonia (*3*). In CPS from *Escherichia coli*, these residues have been identified as Cys269, His353, and Glu355 and the roles of these amino acids during the catalytic cycle have been addressed by site-directed mutagenesis (*4*−*8*). A working model for the chemical mechanism exhibited by the Triad-type amidotransferases is presented in Scheme 1. The kinetic competence of the thioester intermediate in this scheme has been confirmed by rapid-quench experiments (*9*).

Recent results from the X-ray crystallographic analyses of *E. coli* CPS have provided structural support for two of the six complexes depicted in Scheme 1 (*10*−*13*). A ribbon representation of the α,β-heterodimer of CPS is displayed in Figure 1. The initial structure of CPS was solved in the absence of any ligands bound to the amidotransferase domain (*10*). This model, along with that of GMP synthetase (*14*), established the spatial relationships among the critical cysteine, histidine, and glutamate residues in the free enzyme and confirmed the likelihood of their participation in the hydrolysis of glutamine as illustrated in Scheme 1. More recently, the structure of the H353N mutant of CPS was solved after cocrystallization with glutamine (*11*). In this mutant form of the amidotransferase domain, the thioester intermediate with Cys269 was trapped prior to hydrolysis. This structural analysis firmly established the presence of a thioester intermediate during glutamine hydrolysis and identified, for the first time, two additional residues that are involved in the binding and hydrolysis of glutamine. The side chain amide of Gln273 is hydrogen bonded to the α-carboxyl of the glutamyl thioester and O^{γ} of Ser47 is in a position to assist formation of the thioester via stabilization of the incipient oxyanion intermediate.

Here, we provide further structural support for additional complexes that are likely to form during the hydrolysis of glutamine by CPS, namely the Michaelis complex and the tetrahedral intermediate. The Michaelis complex with the native enzyme cannot easily be observed by X-ray crystal-

‡ Department of Biochemistry, University of Wisconsin−Madison, 1710 University Avenue, Madison, Wisconsin, 53705.

§ Department of Chemistry, Texas A&M University, College Station, Texas, 77843

* To whom correspondence should be addressed. Telephone: 608-262-4988. Fax: 608-262-1319. E-mail: Holden@enzyme.wisc.edu.

† This research was supported in part by grants from the NIH (GM55513 to H. M. H., and DK30343 to F. M. R.) and the NSF (BIR-9317398 shared instrumentation grant).

[1] X-ray coordinates have been deposited in the Research Collaboratory for Structural Bioinformatics, Rutgers University, New Brunswick, N. J. (1CS0, 1C30, 1C3O) and will be released upon publication.

[2] Abbreviations: CPS, carbamoyl phosphate synthetase; HEPPS, *N*-2-hydroxyethylpiperazine-*N*′-3-propanesulfonic acid.

10.1021/bi991741j CCC: $18.00
Published on Web 10/30/1999

Scheme 1

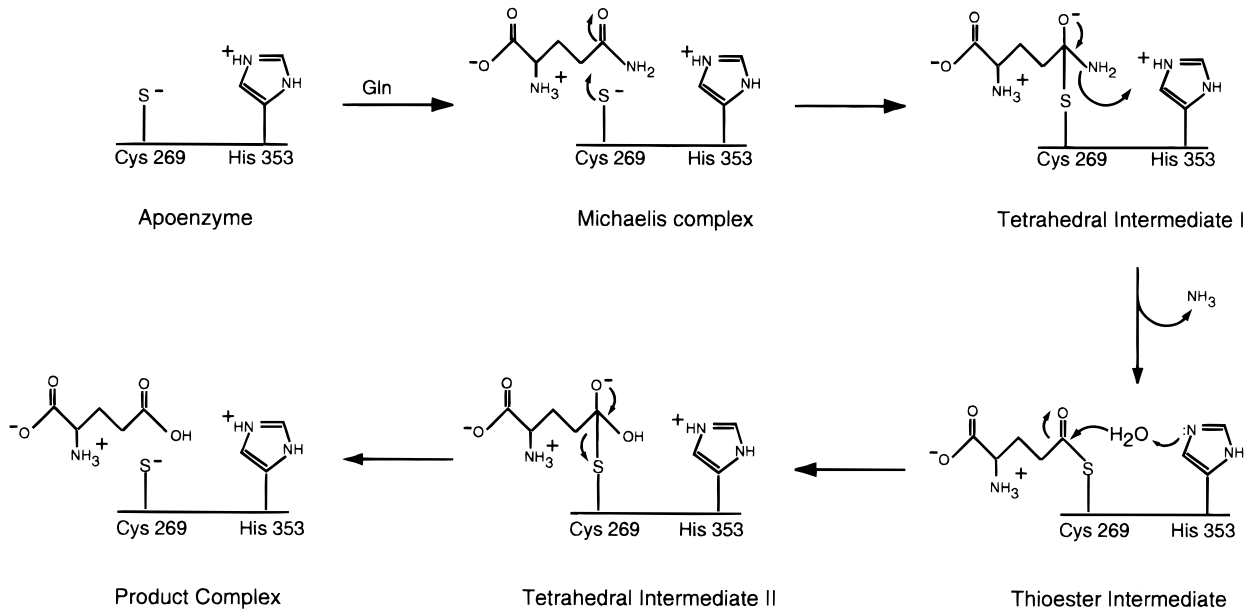

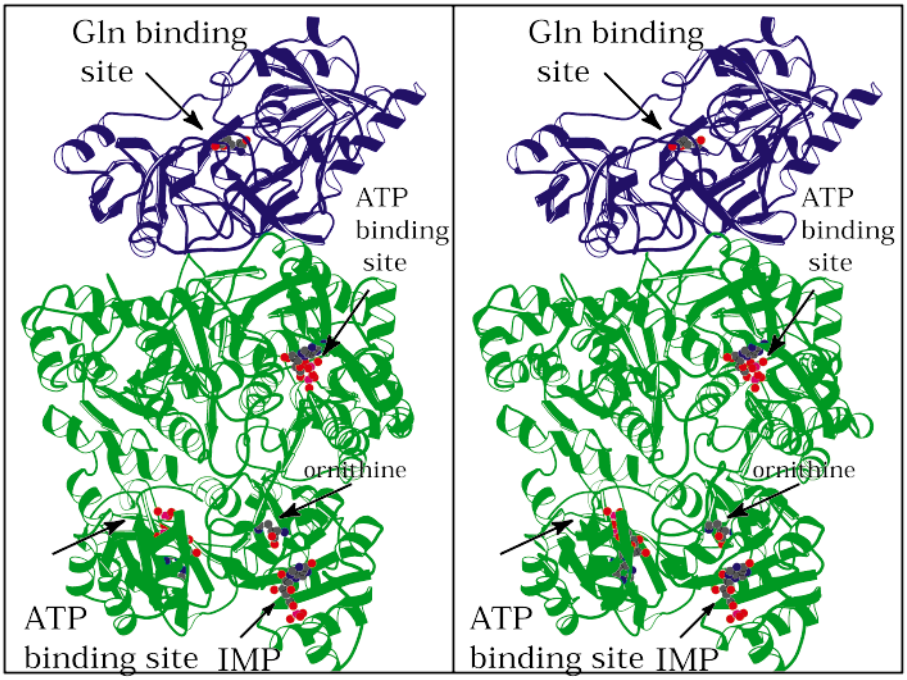

FIGURE 1: Ribbon representation of an α,β-heterodimer of CPS. CPS from *E. coli* consists of two polypeptide chains referred to as the small and large subunits. The small subunit contains both the catalytic machinery necessary for the production of ammonia from glutamine and a molecular tunnel for sequestering the ammonia from the bulk solvent and delivering it to the large subunit. This small subunit is displayed in blue with the glutamine ligand, indicated by the ball-and-stick representation. The large subunit, color-coded in green, is responsible for the production of carbamoyl phosphate from two molecules of Mg^{2+}ATP, one molecule of bicarbonate, and ammonia. The Mg^{2+}ATP moieties are displayed in ball-and-stick representations. In addition, the binding pockets for the allosteric effector molecules, IMP, and ornithine, are also shown.

lographic methods, since there is nothing to prevent the reaction from proceeding through its entirety once glutamine binds to the amidotransferase domain. However, it has been previously demonstrated that when the thiolate anion of Cys269 is substituted with the hydroxyl group of a serine residue, this C269S mutant is unable to hydrolyze glutamine (*4*, *5*). Nevertheless, this site-directed mutant protein binds glutamine to the amidotransferase domain as evidenced by the rate enhancement observed in the overall bicarbonate-dependent ATPase reaction of CPS (*5*). Clearly, the binding of glutamine to the amidotransferase domain of the C269S protein triggers a conformational change in the nearest ATP binding region on the large subunit, which is located nearly 45 Å away. The structure of the C269S protein has now been solved in both the absence and presence of bound glutamine as described here. This mimic of the Michaelis complex of the wild-type enzyme serves as a template to ascertain the magnitude of the conformational changes of active site residues that occur upon the binding of ligands to the amidotransferase domain. In addition, the stereochemistry for attack of the thiolate anion on the planar carboxamide group of glutamine can be determined by the relative

Table 1: X-ray Data Collection Statistics

Data Collection Parameters

	native: L-glutamate γ-semialdehyde	C269S	C269S:L-glutamine
unit cell (Å)			
a	151.7	152.6	152.5
b	163.8	164.6	164.4
c	332.6	332.7	332.6
crystal-to-detector distance (mm)	280	270	290
wavelength (Å)	0.7005	0.7085	0.7005
frame width (deg)	0.40	0.40	0.40
number of frames	450	400	450
exposure time /frame (sec)	17.5	17.0	15.0

Processing/Scaling Statistics

	native:L-Glutamate γ-semialdehyde		C269S		C269S:L-glutamine	
resolution range (Å)	30.0−2.0	2.07−2.00	30.0−2.0	2.07−2.00	30.0−2.10	2.18−2.10
integrated reflections	2729875	210013	2305540	186320	2532077	201948
independent reflections	550694	53688	546635	53813	476527	47060
data completeness (%)	98.7	97.1	97.7	96.8	98.4	97.9
avg I/avg sigma(I)	16.4	2.1	14.8	2.1	16.6	2.2
R-factor (%)	8.9	29.3	8.8	29.1	7.9	28.2

positioning of the bound glutamine with the hydroxyl group of the serine residue substituted for Cys269.

The two forms of the tetrahedral adducts presented in Scheme 1 have been mimicked by complexation with glutamate γ-semialdehyde. In this analogue, the carboxamide side chain of glutamine has been replaced with an aldehyde functional group. Bearne and Wolfenden have demonstrated that this compound is a potent inhibitor ($K_i \sim 10^{-8}$ M) of the reaction catalyzed by glucosamine-6-phosphate synthase (*15*). They have provided convincing evidence to suggest that the inhibitory complex results from the nucleophilic attack of the thiolate anion on the carbonyl group of the free aldehyde. In this paper, we demonstrate that glutamate γ-semialdehyde is a strong inhibitor of the hydrolytic properties of the amidotransferase domain of CPS as well. The structure of the inhibitory complex resembles the expected tetrahedral intermediate depicted in Scheme 1 and further elaborates the manner in which this complex is stabilized by the enzyme. The stereochemistry of this tetrahedral adduct provides additional information on the trajectory of the nucleophilic attack by the thiolate anion on glutamine and the hydrolytic attack on the thioester intermediate. The results presented in this paper will most likely extend to other members of the Triad class of amidotranferases.

MATERIALS AND METHODS

Kinetic Analyses. CPS was purified according to a previously published procedure (*16*). The rates of glutamine hydrolysis and the bicarbonate-dependent ATPase reaction were assayed as described by Post *et al.* (*17*). Glutamic acid γ-semialdehyde was synthesized from hydroxylysine with a yield of 67% (*18*). The aldehyde solution was neutralized to a pH of 7 with KOH immediately before measurement of the inhibitory activity. The data for the inhibition of the glutaminase reaction by the glutamic acid γ-semialdehyde were fitted to eq 1, which describes noncompetitive inhibition. The data for the activation of the bicarbonate-dependent ATPase reaction were fitted to eq 2. In these equations, v is the initial velocity, V_m is the maximal velocity at saturating substrate, K_a is the Michaelis constant for glutamine, I is the concentration of glutamate γ-semialdehyde, A is the concentration of glutamine, K_{ii} and K_{is} are the intercept and slope inhibition constants, respectively, K_i is the activation constant for glutamate γ-semialdehyde, v_o is the initial velocity of the ATPase reaction rate in the absence of the activator, and α is the ratio of the ATPase reaction in the presence and absence of the activator.

$$v = V_m A/(K_a(1 + I/K_{is}) + A(1 + I/K_{ii})) \quad (1)$$

$$v = v_o (K_i + \alpha I)/(K_i + I) \quad (2)$$

Crystallization Procedures. Protein samples employed for crystallization trials were purified as previously described (*6*). Large single crystals were grown at 4 °C by batch from 8% poly(ethylene glycol) 8000, 0.65 M tetraethylammonium chloride, 0.5 mM $MnCl_2$, 100 mM KCl, 1.5 mM ADP, 1.5 mM BeF_3, 0.5 mM L-ornithine, and 25 mM HEPPS (pH 7.4). For preparation of the CPS−tetrahedral mimic, the enzyme was treated overnight at 4 °C with a 20 mM solution of glutamate γ-semialdehyde that had been neutralized to pH 7.0 with KOH. For the C269S−glutamine complex, 10 mM L-glutamine was included in the crystallization buffer. Once the crystals reached dimensions of approximately 0.3 mm × 0.3 mm × 0.8 mm, they were flash-frozen according to previously published procedures (*10*) and stored under liquid nitrogen until synchrotron beam time became available. All of the crystals belonged to the space group $P2_12_12_1$ with typical unit cell dimensions of $a = 152$, $b = 164$, $c = 332$ Å and one complete $(\alpha,\beta)_4$-heterotetramer per asymmetric unit.

X-ray Data Collection and Processing. X-ray data sets for the C269S protein, the C269S−glutamine complex, and the CPS−glutamate γ-semialdehyde complex were collected on a 3 × 3 tiled "SBC2" CCD detector at the Structural Biology Center 19-ID Beamline (Advanced Photon Source, Argonne National Laboratory). The data were processed with HKL2000 and scaled with SCALEPACK (*19*). Relevant data collection statistics are presented in Table 1.

All the structures were solved by Difference Fourier techniques. Each complex was subjected to alternate cycles of least-squares refinement with the software package TNT

Table 2: Refinement Statistics

	native:L-glutamate γ-semialdehyde	C269S	C269S:L-glutamine
resolution limits (Å)	30.0−2.00	30.0−2.00	30.00−2.10
R-factor (overall) %/# rflns	18.6/550694	18.9/546635	18.9/476527
R-factor (working) %/# rflns	18.6/494170	18.9/491971	18.8/426591
R-factor (free) %/# rflns	24.2/56524	24.6/54664	25.8/49936
no. protein atoms	44327	44310	44358
no. heteroatoms	4567	4365	4119
multiple conformations (#)	18	16	27
Weighted Root-Mean-Square Deviations from Ideality			
bond lengths (Å)	0.012	0.012	0.012
bond angles (deg)	2.14	2.26	2.19
trigonal planes (Å)	0.006	0.006	0.006
general planes (Å)	0.011	0.011	0.011
[a]torsional angles (deg)	17.6	17.7	17.8
Solvents			
waters	4176	3987	3666
Mn^{2+} ions	12	12	12
tetraethylammonium ions	4	4	4
ADP moieties	8	8	8
phosphates	5	6	5
ornithines	4	4	4
K^+ ions	37	32	36
Cl^- ions	29	16	16
glutamines	0	0	8

[a] The torsional angles were not restrained during the refinement.

(*20*) and manual adjustment of the model as previously described (*10*). Both the C269S protein model and the CPS−glutamate γ-semialdehyde complex were refined to 2.0 Å resolution. The C269S−glutamine complex was refined to 2.1 Å resolution simply because the crystals did not diffract as well. During the early stages of least-squares refinement, 10% of the X-ray data were excluded for the required calculation of R_{free}. In that all X-ray data are important for the Fourier synthesis, however, these data were ultimately included in the final stages of the refinement and model-building. Relevant refinement statistics are given in Table 2. The *R*-factors listed in Table 2 are based on all measured X-ray data with no sigma cutoffs applied. Note that in each crystalline complex described here the asymmetric unit contains a complete $(\alpha,\beta)_4$-teteramer corresponding to over 5800 amino acid residues. For the sake of simplicity, however, all the data presented in the Results and Discussion section refer to subunit III of the $(\alpha,\beta)_4$-heterotetramer.

RESULTS AND DISCUSSION

Kinetic Results. Glutamate γ-semialdehyde was tested as an inhibitor of the glutaminase activity of CPS. At pH 7.6, it was found to be a noncompetitive inhibitor vs glutamine and the K_{ii} and K_{is} values were 2.8 ± 0.5 and 2.1 ± 0.6 mM, respectively. Since the free aldehyde in solution contributes only 0.05% of the total material, (most of the rest is found in rapid equilibrium as pyrroline-5-carboxylate (*15*)) the corrected values are 1.5 and 1.1 μM for K_{ii} and K_{is}, respectively. Since the K_m value for glutamine in these experiments is 85 μM, it appears that the free aldehyde binds significantly tighter to the protein than glutamine.

The glutamate γ-semialdehyde was also tested as an activator of the bicarbonate-dependent ATPase reaction. This activation of the ATPase reaction is apparently driven by conformational changes that are initiated by binding to the amidotransferase domain and then transmitted to the large subunit. At saturating concentrations of the aldehyde analogue, the rate of the ATPase reaction is enhanced by a factor of 3.3 ± 0.2. The concentration of the aldehyde that provides 50% of this effect is 600 ± 15 μM (the corrected value is 0.3 μM). In contrast, glutamine hydrolysis enhances the steady-state rate of ATP turnover by a factor of 18.

Crystallographic Results. For the sake of clarity, the individual structures of CPS will be discussed in the order given in Scheme 1. Although the structure of the thioester intermediate has been previously described (*11*), it will be presented briefly for the sake of completeness. It was not possible to obtain a structure of the final product complex. Indeed, previous studies have demonstrated that CPS activity is unaffected by concentrations of glutamate up to 100 mM (*21*).

The Apoenzyme. To obtain the structure of CPS with glutamine bound in the small subunit active site, i.e., the Michaelis complex, it was necessary to prepare the site-directed mutant protein C269S. To ensure that this mutant protein was, indeed, a good mimic for the native enzyme, its three-dimensional structure was initially solved in the absence of glutamine. Models of native CPS and the C269S mutant protein superimpose with a root-mean-square deviation of 0.30 Å for all backbone atoms. There are only a few small changes between the two structures and these are confined primarily to the area immediately surrounding the mutation. Shown in Figure 2 is a superposition of these regions in the native and mutant enzymes (*10*). In the mutant protein, O^{γ} of Ser269 lies within hydrogen bonding distance to N of Leu270. This interaction does not occur in the native enzyme. Additionally, His353, part of the catalytic couple, adopts a slightly different conformation in the mutant protein. Specifically the two dihedral angles defined between C^{α} and C^{β} and C^{β} and C^{γ} change by approximately 4° and 32°, respectively. As a result of these changes, $N^{\epsilon 2}$ of His353 lies within 4.3 Å of O^{γ} of Ser269. In the native enzyme,

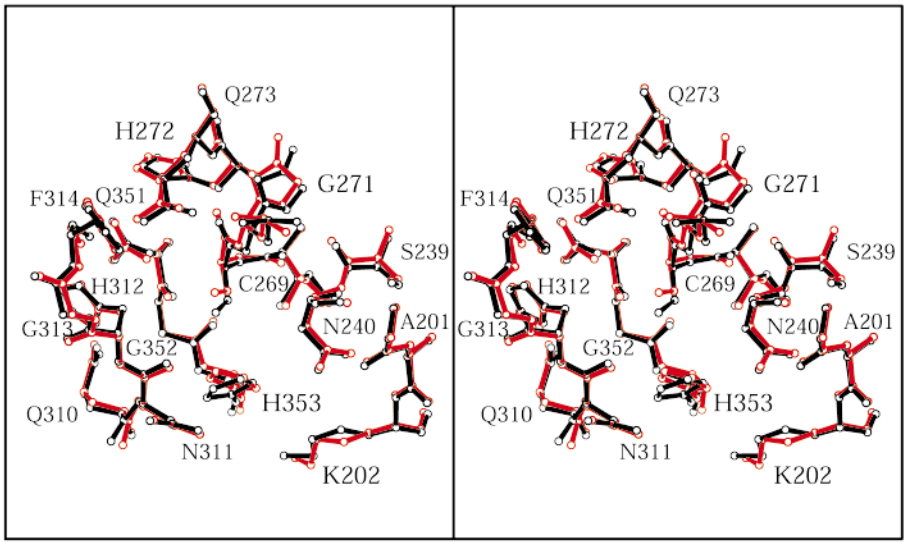

FIGURE 2: Superposition of the native and the C269S protein models near the region immediately surrounding the site of the mutation. The native enzyme is depicted in black while the mutant protein is shown in red.

this distance is approximately 4.1 Å. Other than these minor differences, the two proteins are virtually identical and, as such, the C269S protein proved to be an adequate mimic for studies of the Michaelis complex.

The Michaelis Complex. Shown in Figure 3a is the electron density corresponding to the bound glutamine in the C269S mutant protein. The electron density is very well-ordered and the conformation of the bound ligand is unambiguous. All backbone atoms for the two C269S protein models, with and without bound glutamine, superimpose with a root-mean-square deviation of 0.26 Å.

A cartoon of potential interactions between the glutamine substrate and the protein is given in Figure 4a. Glutamine binds within the small subunit active site such that nucleophilic attack by S^{γ} of Cys269 (replaced with a serine in this case) would occur at the *Si* face leading to a tetrahedral intermediate with the *S*-configuration. The carboxamide moiety of glutamine is hydrogen bonded to CPS via the backbone amide groups contributed by Gly241 and Leu270 and the carbonyl group donated by Asn311. It can be speculated that the backbone amide groups of Gly241 and Leu270 play a pivotal role in the proper positioning of the substrate within the active site. Additionally, these interactions would serve to polarize the carbonyl group and activate C^{δ} of the ligand toward nucleophilic attack by S^{γ} of Cys269. It has been speculated that O^{γ} of Ser47 may be important for stabilizing the developing oxyanion during glutamine hydrolysis (*11*). In the Michaelis complex described here, O^{γ} of Ser47 is located at 4.2 Å from the carbonyl oxygen of the glutamine side chain. The α-amino group of the ligand lies within hydrogen bonding distance to the carbonyl groups of Gly241 and Gly243 and a water molecule. Both the backbone amide groups of Gly313 and Phe314, a water molecule, and $N^{\epsilon 2}$ of Gln273 serve to position the α-carboxylate group of the substrate into the active site. An additional hydrogen bond, not observed in the native enzyme, occurs between O^{γ} of Ser269 and the carbonyl oxygen of the glutamine side chain. Finally, C^{δ} of the substrate, the carbon that would be subject to nucleophilic attack in the native enzyme, lies at 2.8 Å from O^{γ} of Ser269.

The Tetrahedral Intermediates, I and II. The next step in the reaction pathway for glutamine hydrolysis (Scheme 1) is attack by S^{γ} of Cys269 leading to a tetrahedral intermediate. This tetrahedral intermediate was mimicked by employment of glutamate γ-semialdehyde and, as can be seen in Figure 3b, the electron density corresponding to this covalently bound ligand is unambiguous. C^{δ} of the glutamate γ-semialdehyde adopts a tetrahedral configuration with bond angles of ∼111°. The carbon−sulfur bond length is 1.7 Å with this parameter restrained to 1.75 Å during the course of the least-squares refinement. Typical carbon−sulfur bond distances in such compounds range from 1.74 to 1.78 Å as observed in small molecule structures deposited in the Cambridge Data Base. Two structural events occur in the glutamine substrate during the formation of the tetrahedral intermediate: (i) a torsional rotation of ∼130° about the bond defined by C^{α} and C^{β} and (ii) a global movement of the ligand within the active site such that C^{γ} and C^{δ} move by ∼1.7 Å and ∼2.6 Å, respectively.

In the true tetrahedral intermediate, the oxygen of the ligand side chain would be negatively charged. As shown in the cartoon representation in Figure 4b, both the backbone amide groups of Gly241 and Leu270 are positioned to stabilize this oxyanion. In addition, O^{γ} of Ser47 has moved from 4.2 Å to within 3.5 Å of this oxygen as a result of an approximate 30° change in the dihedral angle about the bond defined by C^{α} and C^{β} and a translation of its α-carbon by ∼0.3 Å. The remainder of the glutamate γ-semialdehyde is anchored to the protein in a manner similar to that observed in the Michaelis complex (Figure 4a). The stereochemistry of this aldehyde-based tetrahedral mimic is in the *R*-configuration due to absence of the amide group in the true substrate.

As indicated in Scheme 1, His353 carries a positive charge in both the Michaelis complex and the tetrahedral intermediates. It is assumed that the proton on $N^{\epsilon 2}$ of His353 is donated to the leaving amide group in the first tetrahedral intermediate. Using the coordinates for the glutamate γ-semialdehyde complex described here, it is possible to predict the position of the amide leaving group in the true substrate and, indeed,

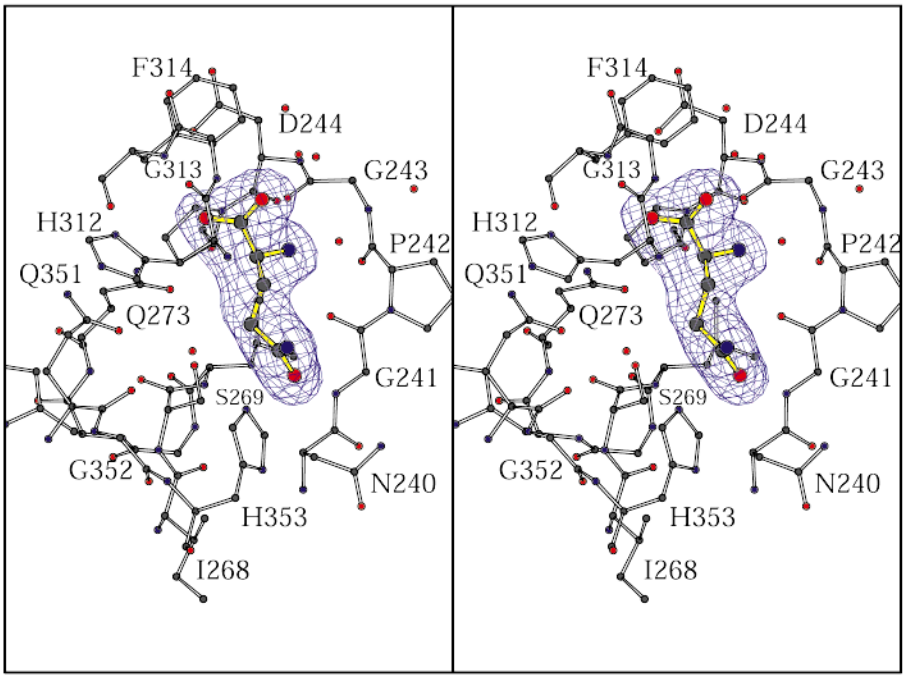

(a)

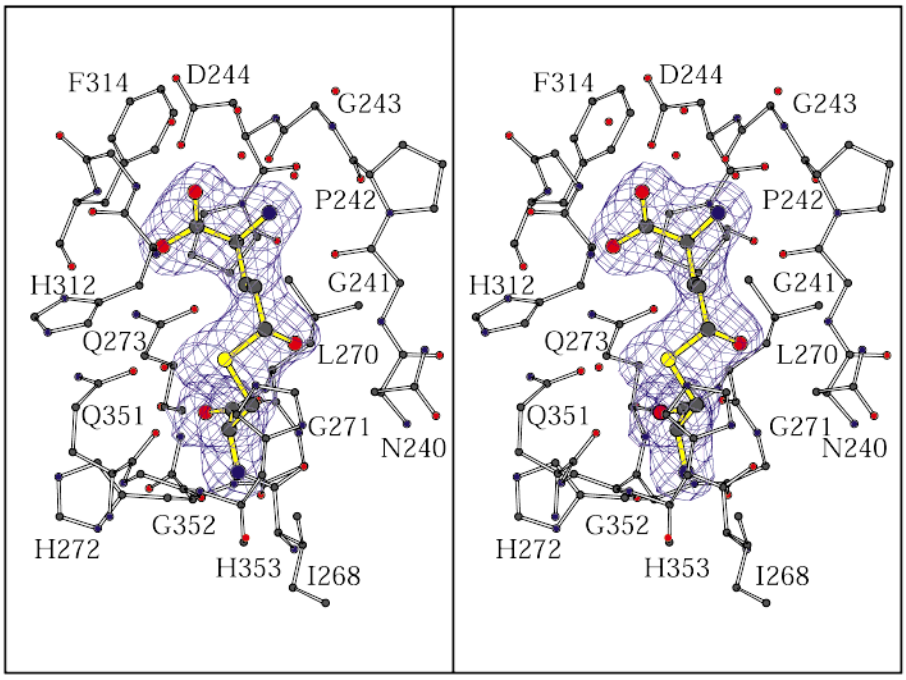

(b)

FIGURE 3: Electron densities corresponding to bound ligands in the small subunit active site. (a) The electron density shown corresponds to the bound glutamine ligand in the C269S protein. The electron density map was contoured at 3σ and calculated with coefficients of the form ($F_o - F_c$), where F_o was the native structure factor amplitude and F_c was the calculated structure factor amplitude. The glutamine ligand was not included in the coordinate file employed for the phase calculations. (b) Electron density corresponding to the glutamate γ-semialdehyde is displayed. The map was contoured at 3σ and calculated in the same manner as described in (a). Coordinates for both the glutamate γ-semialdehyde moiety and Cys269 were omitted from the phase calculations.

this group would be located within hydrogen bonding distance of $N^{\epsilon 2}$ of His353. Furthermore, the amide leaving group is pointed directly toward the molecular tunnel connecting the active site of the small subunit to the first

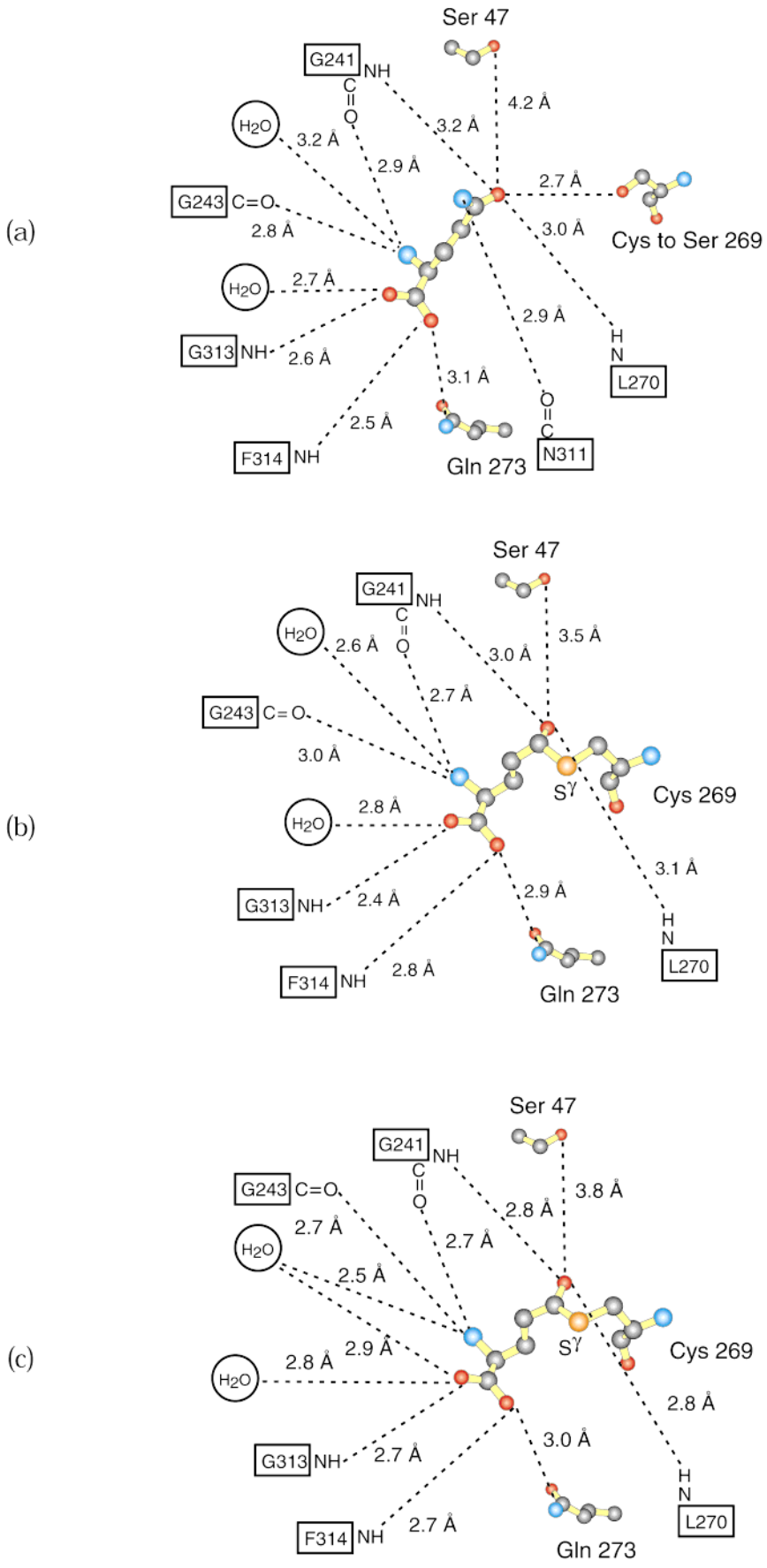

FIGURE 4: Cartoon of hydrogen bonding patterns. Potential hydrogen bonds between the protein and the glutamine substrate, the glutamate γ-semialdehyde moiety, and the glutamyl-thioester intermediate (Protein Data Bank entry 1A9X) are indicated by the dashed lines in (a), (b), and (c), respectively. Distances indicated are in Angströms (Å).

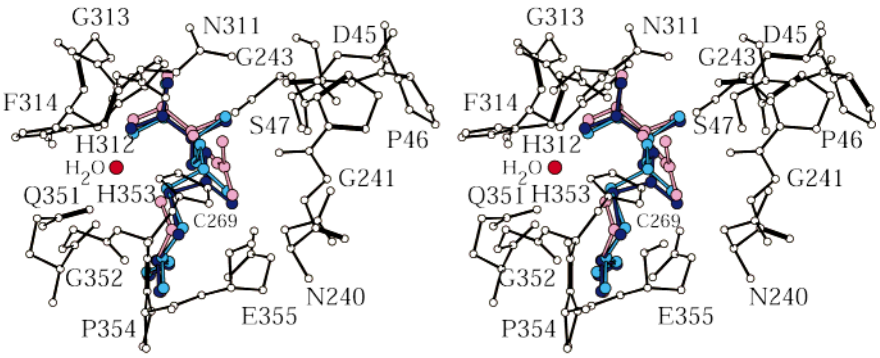

FIGURE 5: Superposition of ligands within the active site of the small subunit. The glutamine, glutamate γ-semialdehyde moiety, and glutamyl-thioester intermediate (Protein Data Bank entry 1A9X) are depicted in pink, light blue, and dark blue, respectively. Note the change in hybridization of C^{δ} from tetrahedral (glutamate γ-semialdehyde) to trigonal (glutamyl-thioester).

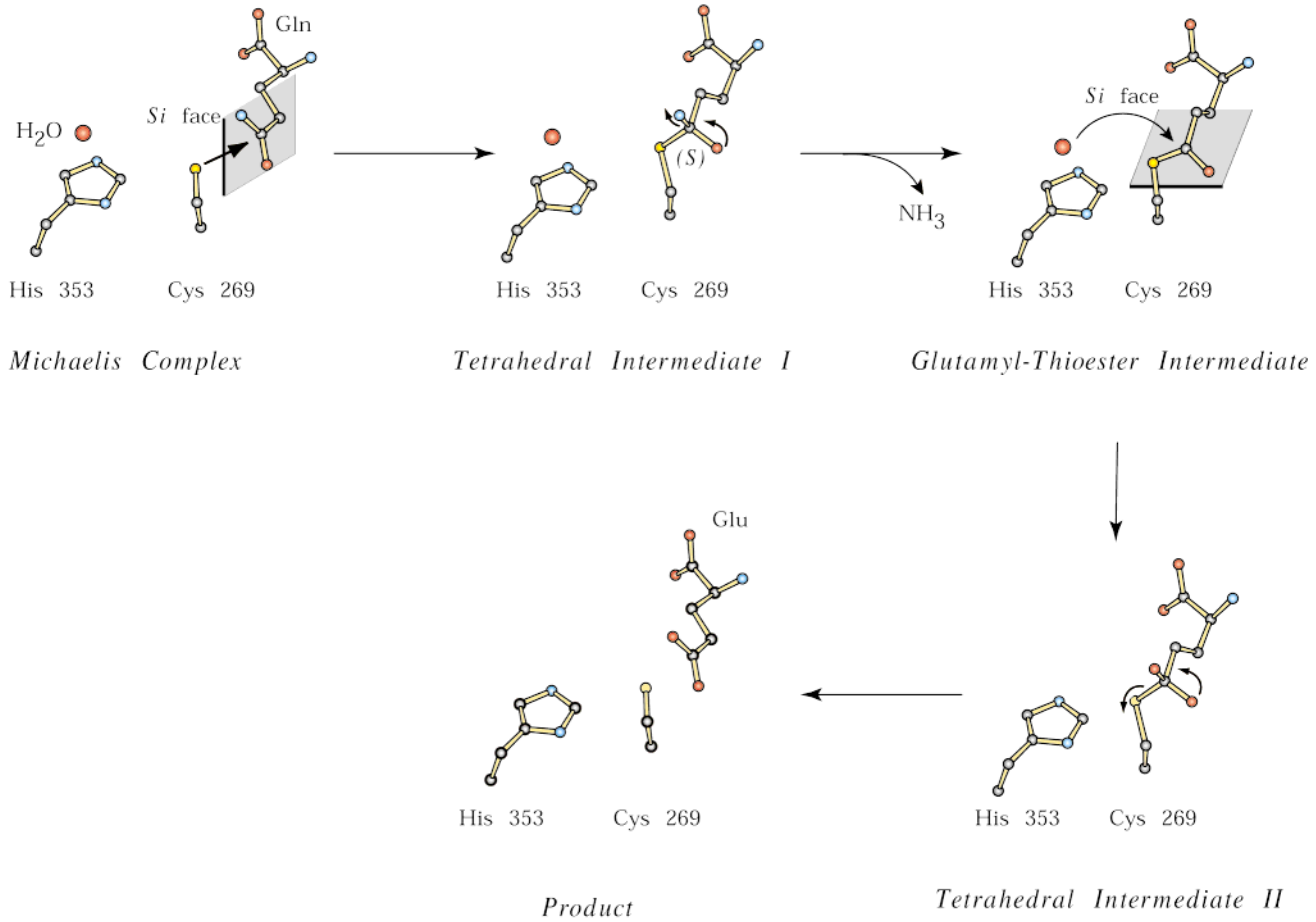

FIGURE 6: Stereochemistry of the reaction pathway for glutamine hydrolysis. The stereochemistry presented is based on the high-resolution X-ray crystallographic structures of the C269S−glutamine, CPS−glutamate γ-semialdehyde, and H353N−glutamyl-thioester complexes.

Mg^{2+}ATP binding pocket of the large subunit. Other than the immediate changes in the small subunit, the Michaelis complex and the tetrahedral intermediate models are virtually identical such that all backbone atoms superimpose with a root-mean-square deviation of 0.26 Å.

The Glutamyl-Thioester Intermediate. For this snapshot along the reaction pathway, the site-directed mutant H353N was prepared and crystallized in the presence of glutamine (*11*). Using this site-directed mutant protein, it was possible to trap the glutamyl-thioester intermediate in the active site of the small subunit. As can be seen in Figure 4c, the hydrogen bonding pattern around the glutamyl thioester moiety is very similar to that observed for the tetrahedral intermediate. As expected, the geometry around C^{δ} of the ligand approaches sp^2 hybridization with bond angles of ~120°. Both the glutamyl-thioester intermediate and the glutamate γ-semialdehyde have similar conformations, the only significant difference being the change in hybridization about their respective C^{δ} atoms. This change from sp^3 to sp^2 hybridization results in the movement of C^{δ} by approximately 1.0 Å. Other than this change, the models for the glutamyl-thioester intermediate and the tetrahedral mimic superimpose with a root-mean-square deviation of 0.34 Å for all backbone atoms.

In both the Michaelis complex and the tetrahedral intermediate model, there is a water molecule lying within

hydrogen bonding distance to $N^{\epsilon 2}$ of His353. This water is also present in an identical location in the glutamyl-thioester intermediate structure even though His353 was replaced with an asparagine residue. Here, it lies within 2.5 Å of $N^{\delta 2}$ of Asn353 and 5.0 Å of C^{δ} of the ligand. It can be speculated that this is, indeed, the water molecule indicated in Scheme 1 that, via its interaction with the imidazole ring of His353, conducts a nucleophilic attack at C^{δ} of the glutamyl-thioester moiety to produce the second tetrahedral intermediate. This solvent molecule is positioned to attack the *Si* face of the glutamyl-thioester intermediate.

Stereochemistry of the Overall Glutaminase Reaction. A close-up view of the three distinct chemical species bound within the small subunit active site is shown in Figure 5 and a cartoon summarizing the stereochemistry of the glutaminase reaction is given in Figure 6. As indicated, glutamine binds within the active site such that its carboxamide group is attacked at the *Si*-face by the thiolate of Cys269. This nucleophilic attack leads to a tetrahedral intermediate with the *S*-configuration. Expulsion of the amide group, aided by proton donation from His353, results in the formation of the second intermediate, the glutamyl-thioester moiety. This entity is subsequently attacked at its *Si*-face by a water molecule, thereby producing the second tetrahedral intermediate. Glutamate is formed upon collapse of this second tetrahedral intermediate.

From the X-ray crystallographic results presented here, it has been possible to describe the overall stereochemistry of glutamine hydrolysis for the Triad class of amidotransferases. What cannot be determined from these studies, however, are the associated structural perturbations that occur and are transmitted to the large subunit upon the binding and hydrolysis of glutamine. Clearly, the three active sites of CPS must communicate in such a manner that ammonia production in the small subunit occurs only at the appropriate moment for its subsequent reaction with the carboxyphosphate intermediate generated in the first active site of the large subunit. This signaling is especially critical in light of the fact that the half-life for the carboxyphosphate intermediate has been estimated to be approximately 70 ms (*22*). Each one of the complexes described here was crystallized in the presence of Mn^{2+}ADP and ornithine. The stereochemical course of glutamine hydrolysis determined in this investigation is unambiguous and is unaffected by the presence or absence of allosteric activators. It is known, however, that replacement of His353 in the small subunit with an asparagine residue results in a form of CPS that is unable to employ glutamine as a substrate yet still binds the ligand as judged by the rate enhancement of the bicarbonate-dependent ATPase reaction of the large subunit *(5)*. Clearly, even though ammonia was not produced at an appreciable rate in this site-directed mutant protein, there was still intramolecular signaling occurring between the large and small subunit active sites. To more fully address the magnitude of such molecular communications that occur upon glutamine hydrolysis, it will be necessary to crystallize CPS in the absence of ligands such as ornithine and Mn^{2+}ADP. This work is currently in progress.

ACKNOWLEDGMENT

We thank Dr. W. W. Cleland for critically reading this manuscript. Use of the Argonne National Laboratory Structural Biology Center beamlines at the Advanced Photon Source was supported by the U. S. Department of Energy, Office of Energy Research, under contract no. W-31-109-ENG-38.

REFERENCES

1. Zalkin, H., and Smith, J. L. (1998) *Adv. Enzymol. Relat. Areas. Mol. Biol. 72*, 87−144.
2. Piette, J., Nyunoya, H., Lusty, C. J., Cunin, R., Weyens, G., Crabeel, M., Charlier, D., Glansdorff, N., and Piérard, A. (1984) *Proc. Natl. Acad. Sci. U.S.A. 81*, 4134−4138.
3. Zalkin, H. (1993) *Adv. Enzymol. Relat. Areas Mol. Biol. 66*, 203−309.
4. Rubino, S. D., Nyunoya, H., and Lusty, C. J. (1987) *J. Biol. Chem. 262*, 4382−4386.
5. Mullins, L. S., Lusty, C. J., and Raushel, F. M. (1991) *J. Biol. Chem. 266*, 8236−8240.
6. Miran, S. G., Chang, S. H., and Raushel, F. M. (1991) *Biochemistry 30*, 7901−7907.
7. Hewagama, A., Guy, H. I., Chaparian, M., and Evans, D. R. (1998) *Biochim. Biophys. Acta 1388*, 489−499.
8. Huang, X., and Raushel, F. M. (1999) submitted to *Biochemistry*.
9. Miles, B. W., Banzon, J. A., and Raushel, F. M. (1998) *Biochemistry 37*, 16773−16779.
10. Thoden, J. B., Holden, H. M., Wesenberg, G., Raushel, F. M., and Rayment, I. (1997) *Biochemistry 36*, 6305−6316.
11. Thoden, J. B., Miran, S. G., Phillips, J. C., Howard, A. J., Raushel, F. M., and Holden, H. M. (1998) *Biochemistry 37*, 8825−8831.
12. Thoden, J. B., Wesenberg, G., Raushel, F. M., and Holden, H. M. (1999) *Biochemistry 38*, 2347−2357.
13. Thoden, J. B., Raushel, F. M., Wesenberg, G., and Holden, H. M. (1999) *J. Biol. Chem.* in press.
14. Tesmer, J. J. G., Klem, T. J., Deras, M. L., Davisson, V. J., and Smith, J. L. (1996) *Nat. Struct. Biol. 3*, 74−86.
15. Bearne, S. L., and Wolfenden, R. (1995) *Biochemistry 34*, 11515−11520.
16. Mareya, S. M., and Raushel, F. M. (1994) *Biochemistry 33*, 2945−2950.
17. Post, L. E., Post, D. J., and Raushel, F. M. (1990) *J. Biol. Chem. 265*, 7742−7747.
18. Williams, I., and Frank, F. (1975) *Anal. Biochem. 64*, 85−97.
19. Otwinowski, Z., and Minor, W. (1997) *Methods Enzymol. 276*, 307−326.
20. Tronrud, D. E., Ten Eyck, L. F., and Matthews, B. W. (1987) *Acta Crystallogr. Sect. A. 43*, 489−501.
21. Raushel, F. M., and Villafranca, J. J. (1979) *Biochemistry 18*, 3424−3429.
22. Sauers, C. K., Jencks, W. P., and Groh, S. (1975) *J. Am. Chem. Soc. 97*, 5546.

BI991741J